Reprocessing of Suomi NPP CrIS Sensor Data Records to Improve the Radiometric and Spectral Long-Term Accuracy and Stability

Yong Chen, Flavio Iturbide-Sanchez, *Senior Member, IEEE*, Denis Tremblay, David Tobin, Larrabee Strow, Likun Wang, Daniel L. Mooney, David Johnson, Joe Predina, Lawrence Suwinski, Henry E. Revercomb, Ninghai Sun, Bin Zhang, Changyong Cao, Satya Kalluri, and Lihang Zhou

***Abstract*— Since early 2012, the cross-track infrared sounder (CrIS) on board the Suomi National Polar-orbiting Partnership (S-NPP) satellite has continually provided the hyperspectral infrared observations for profiling atmospheric temperature, moisture, and greenhouse gases. In this study, the CrIS sensor data record (SDR) data are improved for climate applications with its fine-tuning of calibration coefficients in an NOAA reprocessing project. A specific software system was developed to reprocess the CrIS SDR. This software system was updated with a new calibration algorithm, nonlinearity, and geolocation to improve the SDR data quality and long-term consistency. The calibration coefficients are refined with the latest updates, which were used to calibrate the latest operational SDR products and replace those in the engineering packet (EP) in the raw data record (RDR) data stream. The resampling wavelength was updated based on the metrology laser wavelength and resulted in zero sampling error in the spectral calibration. All the historical SDRs (from February 2012 to March 2017) were generated with the same calibration coefficients and same version of the processing software system, resulting in improved accuracy and stability in terms of spectral and radiometric calibration during the CrIS lifetime mission. The quality of the reprocessed CrIS SDR data at nominal spectral resolution (NSR) is assessed in terms of its radiometric and spectral calibration. Comparisons against the operational SDR data are carried out to demonstrate the improved long-term stability of the reprocessed CrIS SDR data. Overall radiometric biases are found to be small and highly stable over the instrument mission, the FOV-to-FOV differences are less than ∼10 mK, and much better than that from the operational SDR data. It is shown that the CrIS metrology laser wavelength varies within 4 ppm as measured by the neon calibration system. The reprocessed SDR data have spectral errors less than 0.5 ppm, which is much better than the operational SDR data with about 4 ppm. This baseline version of the reprocessed SNPP CrIS SDR data is suitable for long-term climate monitoring and model assessments and can provide an infrared reference observation to assess other narrow- or broadband infrared instruments' calibration accuracy.**

***Index Terms*— Accuracy and stability, calibration, cross-track infrared sounder (CrIS), radiometric and spectral calibration, sensor data record (SDR) reprocessing.**

Manuscript received September 8, 2020; revised January 19, 2021; accepted February 9, 2021. This work was supported by the National Oceanic and Atmospheric Administration JPSS Office under Contract ST133017CQ0050. *(Corresponding author: Yong Chen.)*

Yong Chen, Flavio Iturbide-Sanchez, Changyong Cao, and Satya Kalluri are with the Center for Satellite Applications and Research, National Environmental Satellite, Data, and Information Service (NESDIS), National Oceanic and Atmospheric Administration, College Park, MD 20740 USA (e-mail: yong.chen@noaa.gov; flavio.iturbide@noaa.gov; changyong.cao@noaa.gov; satya.kalluri@noaa.gov).

Denis Tremblay and Ninghai Sun are with the Global Science and Technology, Inc., Greenbelt, MD 20770 USA (e-mail: denis.tremblay@noaa.gov; ninghai.sun@noaa.gov).

David Tobin and Henry E. Revercomb are with the Space Science and Engineering Center, University of Wisconsin, Madison, WI 53706 USA (e-mail: dave.tobin@ssec.wisc.edu; hank.revercomb@ssec.wisc.edu).

Larrabee Strow is with the Department of Physics, University of Maryland at Baltimore County, Baltimore, MD 21250 USA (e-mail: strow@umbc.edu).

Likun Wang and Bin Zhang are with the Earth System Science Interdisciplinary Center, University of Maryland, College Park, MD 20740 USA (e-mail: likun.wang@noaa.gov; bin.zhang@noaa.gov).

Daniel L. Mooney is with the Massachusetts Institute of Technology Lincoln Laboratory, Lexington, MA 02421 USA (e-mail: mooney@ll.mit.edu).

David Johnson is with the NASA Langley Research Center, Engineering Directorate, Hampton, VA 23681 USA (e-mail: david.g.johnson@nasa.gov).

Joe Predina is with Logistikos Engineering LLC, Fort Wayne, IN 46845 USA (e-mail: joe.predina@logistikosengineering.com).

Lawrence Suwinski is with L3Harris Technologies, Inc., Fort Wayne, IN 46818 USA (e-mail: lawrence.suwinski@l3harris.com).

Lihang Zhou is with Joint Polar Satellite System (JPSS), NOAA/NESDIS, Greenbelt, MD 20771 USA (e-mail: lihang.zhou@noaa.gov).

Color versions of one or more figures in this article are available at https://doi.org/10.1109/TGRS.2021.3060639.

Digital Object Identifier 10.1109/TGRS.2021.3060639

NOMENCLATURE

AIRS	Atmospheric infrared sounder.
BT	Brightness temperature.
BTM	Bit trim mask.
CMO	Correction matrix operator.
CrIS	Cross-track infrared sounder.
CRTM	Community radiative transfer model.
DM	Diagnostic mode.
DS	Deep space.
ECMWF	European Center for Medium-range Weather Forecast.
EP	Engineering packet.
ERA-Interim	ECMWF reanalysis interim.
ES	Earth scene.

FIR	Finite impulse response.
FOR	Field of regard.
FOV	Field of view.
FSR	Full spectral resolution.
FTS	Fourier transform spectrometer.
IASI	Infrared atmospheric sounding interferometer.
ICT	Internal calibration target.
ICV	Intensive calibration and validation.
IDPS	Interface data processing segment.
IFS	Integrated forecasting system.
ILS	Instrument line shape.
IR	Infrared.
JPSS	Joint Polar Satellite System.
LWIR	Long-wave infrared.
MAP	Mapping angle parameter.
MWIR	Middle-wave infrared.
MPD	Maximum path difference.
NL	Nonlinearity.
NOAA	National Oceanic and Atmospheric Administration.
NSR	Nominal spectral resolution.
NWP	Numerical weather prediction.
ppm	Part-per-million.
QC	Quality control.
RDR	Raw data record.
SA	Self-apodization.
SDR	Sensor data record.
S-NPP	Suomi National Polar-orbiting Partnership.
SSM	Scene selection mirror.
SWIR	Short-wave infrared.
TVAC	Thermal vacuum testing.
VIIRS	Visible infrared imaging radiometer suite.

I. Introduction

THE CrIS is an FTS on board the S-NPP satellite, which was launched on October 28, 2011. Since April 19, 2012, the JPSS ground processing system called the IDPS has continuously generated the CrIS SDR and has delivered it to user communities.

CrIS measures the spectrum in three IR bands simultaneously: LWIR band at 650–1095 cm^{-1}, MWIR band at 1210–1750 cm^{-1}, and SWIR band at 2155–2550 cm^{-1}. For each scan, CrIS collects 30 ES, 2 DS, and 2 ICT FORs by an arranged 3×3 detector array (or nine FOVs). It provides 1305 channels in the NSR mode for sounding the atmosphere with a spectral resolution at 0.625, 1.25, and 2.5 cm^{-1} at three bands, respectively. The CrIS instrument can also be operated in the FSR mode, in which the MWIR and SWIR band interferograms are recorded with the same maximum optical path difference as the LWIR band and with a spectral resolution of 0.625 cm^{-1} for all three bands (total 2211 channels) [1].

Measurements from hyperspectral IR sensors such as CrIS, the IASI, and the AIRS provide critically important temperature and water vapor information for improving NWP forecast results [2]–[4] and are becoming a significant part of the long-term climate record [5], [6]. These sensors can also be used as space references to calibrate and validate other IR sounders [7]–[9]. All these applications require hyperspectral IR measurements with high and stable calibration accuracy.

Previous studies have demonstrated that CrIS SDR data have high calibration accuracy in radiometric [10], [11], spectral [12], [13], and geometric calibration [14], [15], as well as excellent noise performance [16], [17]. All of those make the SDR data an exceptional asset for weather applications. Nevertheless, the operational IDPS CrIS SDR data quality and calibration accuracy were continuously improved due to the algorithm and software improvements, especially during the ICV period (before February 20, 2014). While the operational SDR data that is produced by IDPS is of adequate quality for weather prediction, it can be further refined so that the subtle climate signal can be captured and analyzed. Therefore, it becomes very necessary to reprocess the CrIS SDRs data with the fine-tuned calibration coefficients and all the major software improvements to provide an improved and consistent new data set for climate and other important applications.

In this article, S-NPP CrIS SDR is reprocessed in an NOAA reprocessing project during the period from February 21, 2012 to March 8, 2017. This article is organized as follows. Section II summarizes all the software improvements and the updates of the calibration coefficients in the reprocessing system. The improvements of SDR overall data quality, radiometric and spectral accuracy and stability in the reprocessed SDR are presented in Section III. Section IV concludes the article.

II. Improvements in CrIS SDR Reprocessing System

Before S-NPP CrIS SDR products reached validated status on February 20, 2014, the calibration coefficients in EP, SDR algorithm and software were continuously refined and improved. During the ICV phase, the SDR product was validated and released to the public users at three maturity levels, named Beta, Provisional, and Validated, respectively. The Beta product is an early released product. At this maturity level, the product is minimally validated and may still contain significant errors. The Provisional product is an improvement over the Beta product, but it may not be optimal and incremental improvements are still occurring. At the validated maturity level, the SDR product is well-calibrated and validated, and uncertainties are characterized over a range of representative conditions. Table I lists important developments during ICV and after validated maturity until June 7, 2017, for EP version 37 upload and IDPS Block 2.0 Mx1 operational. Below we will describe their significances in improving SDR product quality in five aspects: calibration algorithm improvements, spectral calibration improvements, update of NL coefficients, update of geolocation MAPs, and other calibration parameters and software improvements. The reprocessing software system and calibration coefficients are built upon from these improvements.

A. Calibration Algorithm Improvements

The ES view measurements are calibrated radiometrically [18] with two known targets: the hot blackbody ICT,

and the DS view. Following radiometric calibration, spectral correction is then performed [1], [12]. The original operational calibration equation used for CrIS NSR SDR may be written in the following matrix equation form where the sequence of operations proceeds from right to left:

$$S_{\mathrm{ES}} = \mathrm{SA}^{-1}\#F\#\left(f \cdot \frac{C_{\mathrm{ES}}}{C_{\mathrm{ICT}}} \cdot B_{\mathrm{ICT}}\right) \tag{1}$$

where ΔC_{ES} and ΔC_{ICT} are defined as

$$\triangle C_{\mathrm{ES}} = (C_{\mathrm{ES}} - \langle C_{\mathrm{DS}}\rangle)/S_{\psi}, \quad \triangle C_{\mathrm{ICT}} = (\langle C_{\mathrm{ICT}}\rangle - \langle C_{\mathrm{DS}}\rangle)/S_{\psi}.$$

In (1), C_{ES}, C_{ICT}, and C_{DS} are the raw spectra, in digital units, when the instrument views ES, ICT, and DS, respectively; S_{ψ} is the spectral response of the FIR filter, a complex digital bandpass filter which is used to reject the out-band signals and its image passband during the Fourier transform process. The quantities inside of the angled brackets <> correspond to the averaged ICT or DS raw spectra within a four-minute, 30-scan calibration moving window. The main purpose of using the average of the ICT and DS views in the calibration process is to reduce the calibration target noise uncertainty. The function f represents the post radiometric calibration filter, which is used to suppress out-of-band noise amplification that occurs as a result of the $\triangle C_{\mathrm{ES}}/\triangle C_{\mathrm{ICT}}$ operation. This is necessary so that subsequent mathematical operations associated with spectral correction and spectral resampling do not introduce noise artifacts into the final result.

The CrIS instrument uses laser metrology for interferogram sampling that is calibrated by an on-board neon gas emission source [12], [13]. This provides calibration knowledge used to perform spectral correction and spectral resampling. F and SA^{-1} are the spectral resampling and SA correction matrices in (1), respectively. B_{ICT} represents the ICT radiance spectrum calculated on channel grid centers that exist in the CrIS system prior to spectral correction. Due to slight spectral offsets unique to each CrIS FOV that exist prior to spectral correction, then the B_{ICT} radiance is calculated uniquely for each CrIS FOV to compensate for this effect.

In (1), the radiometric calibration, $(\Delta C_{\mathrm{ES}}/\Delta C_{\mathrm{ICT}}) \cdot B_{\mathrm{ICT}}$, is performed prior to the spectral calibration. This approach has three shortcomings that can be eliminated by reversing the order of calibration operations so that spectral correction/resampling is performed prior to radiometric calibration. The first shortcoming is that B_{ICT} must be empirically corrected for any off-axis FOV specific spectral shift as previously discussed when (1) is used. Second, out-of-band noise amplification must be mitigated prior to performing spectral correction when (1) is used. Last and most importantly, the spectral distortions introduced by the FTS measurement hardware act upon an input spectrum that is first optically and electrically filtered by the instrument responsivity function. Thus, the spectral correction would best be performed on this native spectrum prior to the removal of the instrument responsivity function that normally occurs when calculating $(\Delta C_{\mathrm{ES}}/\Delta C_{\mathrm{ICT}}) \cdot B_{\mathrm{ICT}}$ as part of the radiometric calibration. As a result, processing with (1) has resulted in spectral ringing artifacts, which are defined as spectral oscillations present in the un-apodized output SDRs [19]. It has been found that the ringing artifacts exceed the magnitude of nominal Sinc ILS ringing and that these ringing artifacts also depend on the optical path difference sweep direction [1], [19]. Ringing artifacts also increase for larger off-axis FOV angles. The classical approach for reducing these ringing artifacts is to apply an apodization function (such as Hamming) to SDRs.

To effectively reduce the ringing artifacts in the CrIS SDRs, a new calibration approach (2) was proposed by switching the order of radiometric calibration and spectral calibration [1], [20]. The new approach changes the order of spectral calibration and spectral resampling ($F\#f\#\mathrm{SA}^{-1}$) and then first applies this to a phase-corrected raw ES spectrum given by $(C_{\mathrm{ES}}/C_{\mathrm{ICT}}) \cdot |C_{\mathrm{ICT}}|$. This is represented in the numerator of (2) where matrix operations progress from right to left. Similarly, the denominator of (2) performs spectral correction separately on the phase-corrected ICT reference $|C_{\mathrm{ICT}}|$ and does so using the same order of operations as the numerator. The division of numerator by denominator is performed last and this accomplishes the radiometric calibration as the next to last step. The radiometric scale is then provided by multiplying this result by $B_{\mathrm{ICT,req}}$ to complete the radiometric calibration of the spectrum:

$$S_{\mathrm{ES}} = B_{\mathrm{ICT,req}} \cdot \frac{F\#f\#SA^{-1}\#\left(f \cdot \frac{\triangle C_{\mathrm{ES}}}{\triangle C_{\mathrm{ICT}}} \cdot |\triangle C_{\mathrm{ICT}}|\right)}{F\#f\#\mathrm{SA}^{-1}\#(f \cdot |\triangle C_{\mathrm{ICT}}|)} \tag{2}$$

$B_{\mathrm{ICT,req}}$ is the ICT radiance spectrum calculated on the user-required spectral resolution grid.

Same as (1), the common phases from the complex spectra are effectively removed based on the radiometric model $(C_{\mathrm{ES}}/C_{\mathrm{ICT}}) \cdot |C_{\mathrm{ICT}}|$[18]. Different from (1), the phase-corrected, spectrally corrected and spectrally resampled instrument responsivity function is implicitly included in (2) as represented by the denominator term combined with $B_{\mathrm{ICT,req}}$. It acts as a filter to preserve the raw spectrum shape determined by the instrument optics system. The SA effect to the raw spectrum is to spread the radiance to lower frequencies [21], while the SA correction process redistributes the radiance back to the original spectral bins before the SA effect [22]. As a result, the instrument responsivity should be included in the SA correction process. In (2), the responsivity function is not only implicitly included in the SA correction process, but also implicitly removed by the division with the denominator that includes $|\Delta C_{\mathrm{ICT}}|$ with the SA correction process. It was found that compared to the calibration algorithm represented by (1), the improvement in the new calibration algorithm represented by (2) reduces the radiometric calibration inconsistencies among the nine FOVs up to 0.5 K, and reduces the differences between observed and simulated spectra by up to 0.4 K [1]. The calibration equation in (2) was implemented as part of the operational IDPS Block 2.0 Mx1 on April 10, 2017.

B. Spectral Calibration Improvements

The spectral calibration is an essential component in the calibration algorithm [12], [13] and includes three operations: post-filter matrix, resampling matrix, and SA correction matrix. In CrIS SDR processing, the three matrices

TABLE I
MAJOR SOFTWARE AND CALIBRATION COEFFICIENTS UPDATES

Date	Description
31 January 2012	EP v32: Updates of the Programmable Gain Amplifier (PGA) settings and bit trim table (BTM)
2 April 2012	Mx5.3: First IDPS SDR product with geolocation fix
11 April 2012	EP v33: NL coefficients and ILS parameters updates
18 April 2012	CrIS on-orbit FIR digital filter update
19 April 2012	SDR product achieving Beta maturity status
27 June 2012	EP v34: First temperature drift limit updates
15 October 2012	Mx6.3: Geolocation error correction and imaginary QC algorithm in operation
25 October 2012	EP v35: Second temperature drift value changed from 1 to 4; Boresight Yaw and Pitch angle changed
31 January 2013	SDR product achieving Provisional maturity status
22 March 2013	PCT update: MW imaginary QC threshold increased to +/- 0.88 from +/- 0.5
10 July 2013	Mx7.1: Implementation of the full resolution truncation module
14 November 2013	Mx8.0: Time stamp overflow fix; archive reference laser wavelength in CMO file
20 February 2014	Mx8.2: errors fixed in the ILS correction calculations and use a reformulation of the nonlinearity correction equation EP v36: ILS parameters and a2 coefficients corresponding to the new nonlinearity correction equation SDR product achieving Validated maturity status
4 December 2014	CrIS operational on full spectral interferogram mode, IDPS only generated NSR SDR (866, 530, 202), STAR generated the off-line FSR SDR (866, 1052, 799 for the full interferogram data points)
4 November 2015	CrIS extended interferogram with extra data points (874, 1052, and 808) to improve the spectral ringing effect on band edge and evaluate the calibration algorithms
8 March 2017	IDPS Block 2.0 Mx0: IDPS generated both CrIS NSR SDR (CrIS-SDR) and FSR SDR (CrIS-FS-SDR). Both products were using calibration algorithm Eq. (1). The CMO and EngPkt output are separated and resampling wavelength is using the metrology laser wavelength and there is no 2 ppm requirement to rebuild the CMO
10 April 2017	Block 2.0 Mx1: CrIS SDR FOV Remapping; Reorder CrIS Calibration Equations; NSR: algorithm Eq .(1) FSR: algorithm Eq. (2) with 866, 1052, and 799 interferogram data points
7 June 2017	EP 37: mapping angle parameters uploaded to synchronize with the IDPS Block 2.0 Mx1, which included an update to the CrIS SDR FOV mapping

operating for post-filter, resampling, and SA correction are combined into a single matrix [$F\#f\#\mathrm{SA}^{-1}$ in (2)], referred to as CMO.

The post-filter suppresses the noise signal in the guard bands that result from the radiometric calibration, which has no impact on the CrIS spectral accuracy. The SA correction matrix corrects the spectral distortion due to the radiance beam divergence effect from the spectra. Although the SA correction matrix is a function of wavelength, simulations show that it is not very sensitive to the change of the resampling wavelength if the laser wavelength variation is small (less than 100 ppm). For S-NPP, the laser wavelength variation during the life mission is below 4 ppm due to the excellent laser diode temperature control. As a result, the SA correction matrix can be just calculated once in the processing system at the beginning of the mission without further updates. The resampling matrix performs two functions: changing the spectral sampling to the required user resolution, and interpolating the spectrum from the sensor wavenumber grid onto the user-defined wavenumber grid. For CrIS spectra, the spectral resolution is defined as the spectral distance between two adjacent channels. The resampling matrix maps the spectra from the sensor grid to the user grid and therefore the amount of relative spectral error occurring in the raw spectra due to the metrology laser wavelength drifts is the same as that in the user grid after spectral resampling [13]. While the CrIS neon calibration system provides measurements of the laser wavelength periodically roughly once per orbit (109 min), the initial operational spectral calibration algorithm did not update the resampling matrix as often as the neon measurements were carried out. The spectral resampling matrix was only updated when the metrology wavelength drifted more than 2 ppm from the initial metrology laser wavelength. To take the laser wavelength variation into account, the spectral resampling matrix needs to be frequently updated to reflect the changes in the sensor spectral grid. In the updated CrIS SDR reprocessing algorithm, the spectral resampling matrix is recalculated whenever the metrology laser wavelength is updated by the CrIS on-board neon calibration system, which effectively and significantly reduces the spectral sampling error and improves the spectral uncertainty of the CrIS SDR data [13].

The SA correction matrix is strongly dependent on the geometry of the focal plane detectors. The geometry representing the exact alignment of the detectors to the interferometer boresight axis, including FOV size and offset angles, is referred to as ILS. The ILS parameters were initially estimated during the instrument TVAC by analyzing the gas cell measurements. Then, during the ICV period, the ILS parameters were refined by performing analysis of in-orbit Earth view spectra using both relative spectral calibration, with spectra from the center FOV 5 as references, and absolute spectral calibration, with simulated spectra from radiative transfer models [12] as references. Validation results have shown that the relative spectral calibration biases among FOVs are within 1 ppm. This value is small enough that NWP assimilation systems can treat different FOVs as a single system in terms of bias correction. As shown in Table I, the ILS parameters have been updated several times during the ICV period, specifically, in the operational EP v33 (April 11, 2012) and EP v36 (February 20, 2014). Each update improves the spectral accuracy of the operational CrIS SDR radiance products. In the CrIS SDR reprocessing software system,

the ILS parameters defined in the EP v36 are used to generate the reprocessed data.

C. NL Coefficients Update

The instrument NL arises from detectors, analog amplifier section, and analog to digital converter. The CrIS detectors are photovoltaic HgCdTe which produce an electric signal proportional to the radiation absorbed by the detectors. The detector responsivity dominates the instrument NL and this property is susceptible to change when the detectors are subjected to extreme temperature variation. This is particularly observed during TVAC activities, where the detectors are warmed up during inactivity and then cooled down for data acquisition. Extensive analysis of CrIS prelaunch characterization data and of CrIS in-orbit data had been performed to characterize not only the magnitude of the quadratic NL but also the order (quadratic, cubic, etc.) and character of the NL. For the prelaunch data collected during TVAC testing, two types of data were used. The first was DM data which by-passed the normal numerical filtering and decimation processing to retain signal frequencies outside of the normal bandpass so that out-of-band harmonics can be analyzed. The out-of-band harmonics clearly showed that the order of the NL was quadratic and no other signals were observed at out-of-band frequencies which would indicate a cubic or higher-order NL. This observation was validated with normal mode prelaunch data collected for a wide range of scene temperatures from 200 to 310 K. In-orbit, DM data was also collected in the ICV phase to verify the prelaunch findings, and various assessments of the Earth view spectra (e.g. comparisons to other sensors, comparisons to calculated spectra, etc.) were also used. Examples of the DM out-of-band harmonics were shown in [23], and details of the NL assessment were contained in [11]. Last, the NL correction coefficients were refined further by performing analysis of in-orbit Earth view data. During this process, new NL coefficients were adjusted by using the most linear detector as a reference to minimize the radiometric FOV-to-FOV difference [11]. The correction to the detector NL effect is a scaling operation on the raw spectrum by a factor $(1 + a_2 V)$, where a_2 is a detector dependent constant (NL coefficient) and V is the voltage produced solely from detector photon and dark currents, determined dynamically for each spectrum. Details of the NL correction of the CrIS instrument as well as its significance to the instrument radiometric uncertainty were reported in [11]. The NL correction algorithm in the IDPS software system has been updated after February 20, 2014 (corresponding to EP v36), using the new scaling factor of $(1 + a_2 V)$. This differs from the old scaling factor $(1 - a_2 V)$. The correction algorithm update positively impacted the radiometric FOV-to-FOV performance, especially in LWIR channels. After performing radiometric FOV-to-FOV consistent analysis using in-orbit Earth view data, the NL coefficients were refined accordingly. Fig. 1 shows the NL coefficients used in CrIS SDR reprocessing for LWIR and MWIR (red bar) as well as those in EP v33 (black bar) and EP v36 (green bar). The NL coefficients for SWIR can be negligible and currently set to zero. Notice that there are

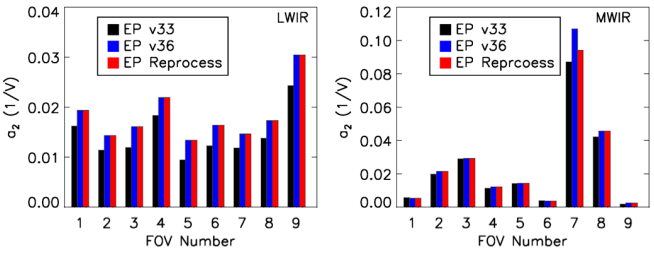

Fig. 1. NL coefficients in CrIS SDR reprocessing for LWIR and MWIR. Notice that there are larger difference between EP v36 and EP v33 for LWIR after adjustment using on-orbit data in order to make the FOV-to-FOV comparison more consistent. For reprocessing, only FOV 7 in MWIR is reduced 12% from EP v36, other coefficients are the same as EP v36.

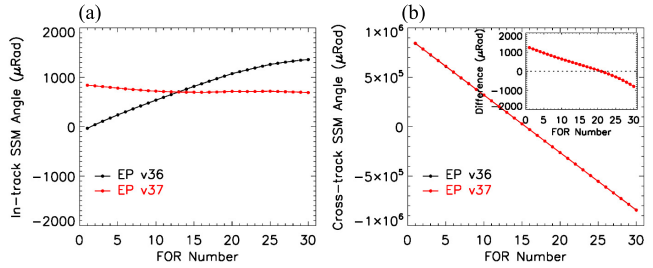

Fig. 2. Comparison of SSM mapping angles in EP v36 and EP v37: (a) in-track and (b) cross-track angles derived from geolocation assessment results as a function of FOR. Notice the angle differences in the cross-track direction are also showed in (b). In the CrIS SDR reprocessing system, the mapping angles in EP v37 are used.

larger differences between EP v36 and EP v33 for LWIR mainly due to the change of the NL scaling factor. In the CrIS SDR reprocessing software system, the updated NL correction algorithm is applied to all the data. Only NL coefficient for FOV 7 at MWIR is reduced by 12% from EP v36 to improve the FOV-to-FOV consistency, other NL coefficients are kept the same as EP v36.

D. Geolocation MAPs Update

The geolocation mapping angles at the instrument-level were measured during the prelaunch test and were set as static values in the EP. These parameters could be optimized and updated to account for the uncertainties of the prelaunch measurements and other on-orbit factors (e.g., such as satellite launch drift, gravity effects, and thermal distortion) to reduce the systematic geolocation errors. To evaluate the postlaunch on-orbit CrIS geolocation performance, the geolocation fields from the SNPP VIIRS image band I5 were used as truth by taking advantage of its high spatial resolution (375 m at nadir), accurate geolocation [15], as well as it is on the same satellite platform. By performing perturbation of the CrIS line-of-sight vectors along the in-track and cross-track directions, an optimal position could be found where CrIS and VIIRS band I5 radiances match most closely. The perturbation angles at this best-matched position can be treated as the CrIS geolocation error. The error characteristics along the scan positions in the in-track and cross-track directions are then used to adjust the CrIS MAPs [24]. Fig. 2 shows the SSM in-track and cross-track direction mapping angles comparison

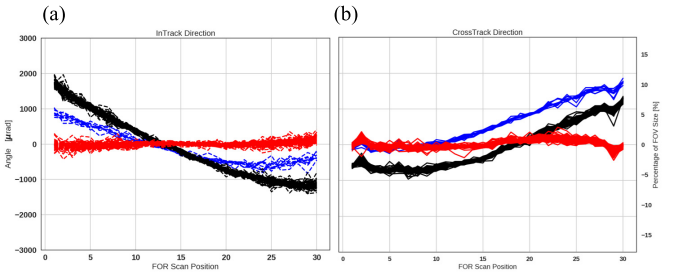

Fig. 3. CrIS Geolocation assessment results using VIIRS image band I5 geolocation as a truth, including (a) the offset angle in the in-track direction and (b) the offset angle in the cross-track direction. Blue curve: MAPs in EP v36 with IDPS Block 2.0 Mx0. Red Curve: MAPs in EP v37 with IDPS Block 2.0 Mx1. Black line: MAPs in EP v36 with IDPS Block 2.0 Mx1. Note that the FOV size is 16 808 μrad, 1000 μrad is approximately 850 m at nadir.

for EP v36 and EP v37. It shows that the angle differences between EP v37 and EP v36 can reach up to ∼1000 μrad in both in-track and cross-track directions. It should be pointed out that the angles shown in Fig. 2 are computed based on geolocation assessment results from the operational IDPS Block 2.0 Mx1 geolocation produced with CrIS SDR FOV remapping correction in the software (see Table I). Fig. 3 shows CrIS geolocation assessment results using VIIRS image band I5 geolocation as a truth, including (a) the offset angle in the in-track direction and (b) the offset angle in the cross-track direction. In this figure, the blue curves are for the results using the MAP defined in EP v36 with IDPS Block 2.0 Mx0, and those results represent the operational geolocation error before April 10, 2017. The red curves are for the results using MAP in EP v37 with IDPS Block 2.0 Mx1, which includes an update to the CrIS SDR FOV mapping correction and synchronizes with the MAP in EP v37 after June 7, 2017, and represent the operational geolocation error after June 7, 2017. The black curves are for the results using the MAP in EP v36 with IDPS Block 2.0 Mx1, and represent the geolocation error from the mismatch period between April 10, 2017 and June 7, 2017. Note that the detector diameter is 16 808 μrad, and 1000 μrad offset is approximately 850 m at nadir on the Earth's surface. The geolocation accuracy requirement is about 11% of FOV size on the Earth's surface for all scan positions and 1.5 km at nadir. It is found that there is a relatively large error (∼2 km) in the cross-track direction (blue curves) relative to VIIRS at the end of the scan in EP v36. With the updated mapping angles in EP v37, the geolocation accuracy is greatly improved for all scan positions with less than 0.25 km. In the CrIS SDR reprocessing software system, the mapping angle parameters from EP v37 are used.

E. Other Significant IDPS Software and Calibration Coefficients Updates

Table I lists the important S-NPP SDR algorithm and software improvements and calibration parameter refinement until June 7, 2017. The detailed descriptions of the S-NPP CrIS postlaunch developments in SDR software and calibration coefficients updates before Provisional status were given in [10], and will not be repeated here. Below we briefly describe their significances in improving SDR product quality after the SDR product had achieved Provisional status on January 31, 2013.

On October 15, 2012, a new QC algorithm was implemented in the SDR software to invalidate a spectrum if the magnitude of its imaginary radiance values exceeds a predefined threshold. The purpose of this QC algorithm implementation is to identify corrupted spectra caused by software, SDR processing errors, or observation anomalies before the errors can be fixed. On March 2013, the MWIR imaginary QC threshold was increased from 0.5 to 0.88 to effectively reduce the false alarm cases for some good spectra over hot scenes such as deserts. The new optimized threshold of 0.88 was chosen by analyzing these hot scenes and to separate the false alarm cases with slight larger imaginary radiances exceeding the old threshold of 0.5 from the saturated cases with distorted spectra. On July 10, 2013, an important module to truncate the CrIS extended interferograms into nominal interferograms became operational. This module makes it possible for CrIS SDR software to run in two modes, one is for NSR SDR product, and another is for FSR SDR. To unpack the RDR data in the interferogram, the BTM and calibration coefficients information stored in the EP must be available. The possibility of the SDR anomaly at the restart of the SDR process without the calibration coefficients and BTM was eliminated by finding and placing the EP at the first scan in the 30-scan calibration moving window. On November 14, 2013, the timestamp overflow issue for scan time was fixed by replacing the data type unsigned integer 32 with unsigned integer 64 to hold a big integer value, and the reference laser wavelength used for CMO calculation was archived in output/input CMO file. On February 20, 2014, software updates were implemented to fix errors found in the ILS correction calculations and to use a new reformulation of the NL correction equation. The original software assumed the FOV 5 is centered at the optical axis, which is not exactly right. By ignoring the offset of the FOV center and using the wrong radius to calculate the ILS correction, resulting in 1.4 and 2.0 ppm errors in the FOV 5 spectral calibration for LWIR and MWIR bands, respectively. This affected other FOVs' relative spectral calibration accuracy since FOV 5 is used as a reference for all other FOVs. The method to determine the offset of FOV 5 and other FOVs focal plane parameters was detailed in [12]. The initial focal plane parameters and the Neon lamp effective wavelength were determined by using TVAC gas cell data, and refined by using the on-orbit observation. After fixed the software bug, the ILS parameters were refined and updated in EP v36 (see also Section II-B). The overall quality flag was updated to handle the short granule (containing less than four scans data) and missing packets. To accompany the software updates of the ILS and NL correction equations, small adjustment of ILS parameters and a_2 coefficients corresponding to the new NL correction equation were updated with EP v36 in the RDR data stream. Although there is 4 h gap between the software update and calibration coefficients update, the SDR product achieved Validated maturity status on the same day.

On December 4, 2014, the CrIS instrument operated on full spectral interferogram mode with data points of 866, 1052, and 799 for the three bands, respectively. While IDPS still generated NSR SDR using the truncation module to truncate the interferogram data points to 866, 530, 202 for the three instrument spectral bands, NOAA/STAR began the successful generation of the off-line SNPP CrIS SDR data at FSR SDR, that consisted of data with 0.625 cm^{-1} spectral resolution for all three bands. The generated data was made available for users and the science community. On November 4, 2015, the CrIS instrument further extended the interferogram data points for LWIR and SWIR to 874 and 808, respectively. The purpose of this extension is to reduce the spectral ringing effect on band edge by using these extra data points, and to evaluate and to improve the calibration algorithm. On March 8, 2017, the IDPS Block 2.0 Mx0 generated for the first time both CrIS NSR SDR (CrIS-SDR) product and CrIS FSR SDR product (CrIS-FS-SDR). Both products use the same calibration algorithm represented by (1). However, the output files for CMO (Correct-Matrix-AUX, only containing the reverse SA matrix) and Engineer Packet backup (ENGPKT-BACKUP-AUX) are separated and the resampling matrix uses the metrology laser wavelength and there is no 2 ppm requirement to rebuild the CMO (see Section II-B). On April 10, 2017, a FOV geolocation remapping correction and a new CrIS calibration algorithm for FSR SDR, represented by (2), were used as part of the IDPS Block 2.0 Mx1 operational processing system. On June 7, 2017, the geolocation MAPs were updated in EP v37 to synchronize with the FOV geolocation remapping correction in the IDPS Block 2.0 Mx1. With these updates, the CrIS geolocation accuracy improved from 2.0 km to less than 0.3 km for all scan angles in both cross-track and in-track directions (see Fig. 3).

III. Results of CrIS SDR Baseline Reprocessing

As shown in Section II-E, the operational IDPS CrIS SDR data quality is significantly and continuously improved due to the calibration algorithm and software improvements as well as the refinement of the calibration coefficients. This is particularly clear during the ICV period before the SDR product achieved validated maturity status. The inconsistency and potential low stability of the operational IDPS CrIS SDRs during the life-time mission are not suitable for long-term climate trends and other climate applications. In this study, we have developed one specific reprocessing software system similar to IDPS Block 2.0 Mx1 for CrIS NSR SDR reprocessing. This software system is updated with all the latest improvements implemented operationally, such as the calibration algorithm, NL reformation, ILS correction, as well as geolocation FOV remapping. All of them resulted in improvements in the quality of the scientific SNPP CrIS SDR data. The calibration coefficients for the ILS parameters, NL coefficients, and the MAPs are refined with the latest updates as in EP v37 (except for FOV 7 NL coefficient at MWIR) and replace the older ones in the RDR data stream. As a result, all the reprocessed SDRs are generated with the same calibration coefficients and the same version of processing software system during the reprocessing period from February 21, 2012 to March 8, 2017. The improvements from the reprocessed CrIS SDRs are compared against the operational IDPS SDRs, and discussed in detail in this section in terms of overall data quality, long-term radiometric as well as spectra calibration accuracy and stability.

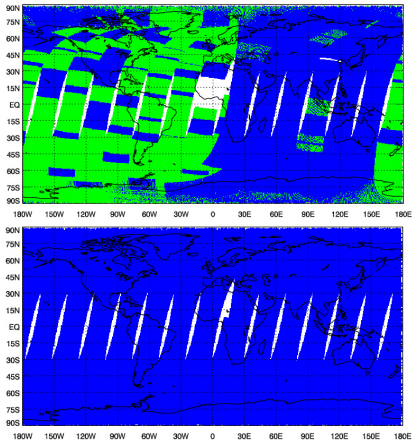

Fig. 4. (Top panel) LWIR band overall quality flag at descending orbits on June 27, 2012, from IDPS SDR. (Bottom panel) Reprocessed SDR. The blue color indicates good overall quality, and the green color degraded overall quality. Note that there are no degraded values and no data gaps in the reprocessed SDR data because the good temperature drift limits and the latest RDR data were used.

A. Overall Data Quality

One of the major improvements in the reprocessed CrIS SDRs is the overall data quality. Due to the operational software bugs and the initial calibration coefficients, which were determined using the prelaunch measurements, there were some issues in the operational IDPS SDR data especially during the ICV period (before February 20, 2014). The processing system was continuously updated to fix bugs and the calibration coefficients were tuned based on the assessments of the on-orbit observations. At the same time, each day there were several repaired RDR granules (each RDR granule contains four scans of data that correspond to 32 s of observations). This anomaly in the RDR data caused data gaps in the operational IDPS SDRs, mainly due to the delay in the arrival of the repaired RDR data and the time requirement for the operational IDPS SDRs to meet the time window in the weather forecast systems. For the reprocessed SDRs, both the software errors and the delay in the RDR granules are resolved by taking advantage of the refined calibration coefficients, improved software, and the usage of the best available RDR data.

Fig. 4 shows the LWIR band overall SDR data quality flag at descending orbits on June 27, 2012, from the IDPS SDR (top panel) and the reprocessed SDR (bottom panel), respectively. The blue color indicates good overall quality, and the green color is for degraded overall quality. It can be seen that there are over 60% of the valid spectra flagged with a degraded status in the operational IDPS SDR due to the excess temperature drifts for ICT and scan baffle. In addition, there

are clearly notable data gaps in the operational IDPS SDR due to the delay issue of the repaired RDR granules. However, in the reprocessed SDR, there are no degraded spectra and no data gaps because the good temperature drift limits and the latest RDR data were used. It shows how the reprocessed data maximizes the availability of CrIS observations as compared to the operational IDPS SDR data.

B. Radiometric Accuracy and Stability

There are three potential methods to assess the CrIS SDR radiometric accuracy, including 1) direct comparison with NOAA-20 CrIS SDR radiance products after January 5, 2018, when the NOAA-20 CrIS instrument went into an operational mode (although there is a 50.7 min orbit separation); 2) comparison with IASI/AIRS using simultaneous nadir overpasses method over polar regions; and 3) comparison with forward radiative transfer model simulation. The first method is not applicable to our reprocessing period ending at March 8, 2017, but could be very useful in the future reprocessing radiometric evaluation to quantify the radiometric difference and create a calibration link between SNPP and NOAA-20 CrIS [25], which is crucial for creating CrIS long-term climate data records. Similar to the first method, the second method could create a calibration link between CrIS and IASI/AIRS to create even longer hyperspectral IR climate data records. However, due to the spatial coverage limitation, we do not use the second method either. Methods 1 and 2 will be a topic for future study to detail the reprocessed CrIS SDR radiometric performance. In this study, we only use the third method that considers the simulated observations as the radiometric reference.

The CrIS radiances are simulated using the CRTM [26]–[28] and the ECMWF 3-h forecast model data as well as ERA-interim data. ERA-Interim is a global atmospheric reanalysis from 1979, continuously updated in real time. The data assimilation system used to produce ERA-Interim is based on a 2006 release of the IFS version Cy31r2. The spatial resolution of the data set is approximately 80 km on 60 vertical levels from the surface up to 0.1 hPa [29]. Different from the ERA-Interim data set generated from one version of IFS, the ECMWF forecast model data set is continuously improved from the IFS version upgrades with better vertical and horizontal resolutions as well as physical processes. To better collocate the observation and simulation spatially and temporally, the forecast/reanalysis of atmospheric and surface fields from the model data set at the neighboring grids are first bilinearly interpolated to the CrIS observational pixel location, and then linearly interpolated to the CrIS observational time. Due to the large errors in modeling land, ice, and snow surface emission and reflection, surface skin temperature, as well as the cloud field, we only consider the clear scenes over the ocean within [60°S, 60°N]. The clear scenes are obtained using a hyperspectral IR cloud detection algorithm, in which the CrIS observed scenes with possible contamination by clouds are effectively removed [13].

Fig. 5 shows the time series of daily mean biases between the CrIS observations from the reprocessed SDR and CRTM simulations using ECMWF forecast (black curve with an open circle, referred to as Bias1) and ERA-interim (red curve with an open circle, referred to as Bias2) over ocean clear scenes at CrIS LWIR channel 10 (655.625 cm^{-1}). The observation minus simulation results are strongly dependent on the input atmospheric profiles and surface conditions. However, this is a strong CO_2 absorption channel with a weighting function peak height around 50 hPa (altitude ∼20 km), from which the majority of energy contributed to the CrIS observed radiance is through the atmospheric emission. One can see that Bias1 has several notable jumps as a function of time. These jumps from this upper CO_2 channel are related to the ECMWF model upgrades, especially related to the changes in the model vertical resolution. For example, on June 25, 2013, the vertical levels were increased from 91 to 137 in ECMWF IFS version cy38r2, with significant improvement on temperature above 100 hPa, resulting in the bias reducing from ∼0.6 to ∼0.2 K. On November 19, 2013, the vertical levels from the ensemble system were increased from 62 to 91 in ECMWF IFS version cy40r1. On March 8, 2016, ECMWF IFS was upgraded to version cy41r2. Notice that the data gap from May 8, 2014 to June 16, 2014 is due to the loss of ECMWF forecast data at NOAA/STAR. Due to these IFS model upgrades, the long-term bias change is ranging from 0.0 to 0.65 K during our assessment period from September 23, 2012 to March 8, 2017. One can see the larger short-term variation from day to day in Bias2 compared to Bias1 due to the coarser vertical resolution and the older IFS version in ERA-interim. However, Bias2 show a significant improvement on long-term stability when using ERA-interim model fields as inputs. There is no obvious radiometric trend in Bias2 during the four-and-half-year reprocessed period. Although ECMWF model output is better to evaluate the short-term radiometric accuracy (smaller variation from day to day), it may not be good for the long-term stability assessment due to the continuous model updates/upgrades. By contrast, the ERA-interim data is a much better choice than ECMWF forecast data for evaluating long-term stability [29].

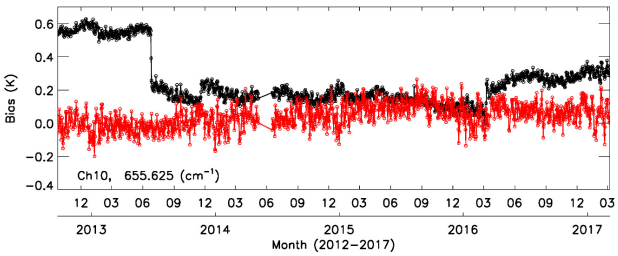

Fig. 5. Time series of daily mean biases between the CrIS observations from reprocessed SDR and CRTM simulations using ECMWF forecast (black curve with open circle) and ERA-interim (red curve with open circle) over ocean clear scenes at CrIS LWIR channel 10 (655.625 cm^{-1}). The jumps in the black curve are related to the ECMWF model upgrades. Notice that the data gap from May 8, 2014 to June 16, 2014 is due to loss of ECMWF forecast data.

Fig. 6 shows the time series of daily mean biases at CrIS MWIR channel 872 (1407.5 cm^{-1}). This water vapor channel has a weighting function peak at a height of around 590 hPa (altitude ∼4.5 km). Bias1 is much smaller (around 0.5 K) than Bias2 (around 1.5 K), indicating that the water

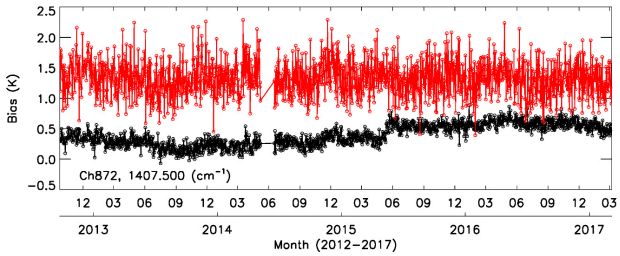

Fig. 6. Same as Fig. 5, but for CrIS MWIR channel 872 (1407.5 cm^{-1}).

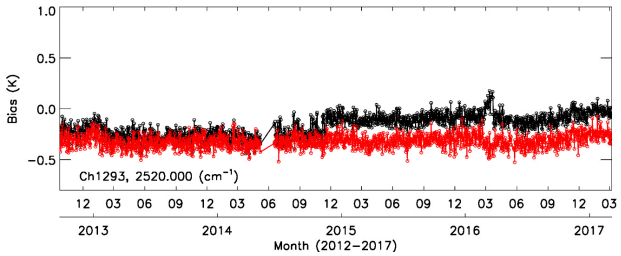

Fig. 7. Same as Fig. 5, but for CrIS SWIR channel 1293 (2520.0 cm^{-1}) and at night time.

vapor information at altitude around 4.5 km from ECMWF forecast data is much better than those from ERA-interim [29]. It should be pointed out that the ERA-interim data has about ∼80 km horizontal resolution and only has 60 vertical levels (compared to ECMWF forecast data with nominal ∼30 km horizontal resolution and 137 vertical levels), while CrIS observation has a ground spatial resolution of 14 km at nadir. This channel is mainly sensing the lower free troposphere where water vapor is abundant and highly dynamic. It shows that Bias1 has a smaller short-term variation than Bias2. However, Bias2 shows better long-term stability than Bias1 by using the same version of model output.

Fig. 7 shows the time series of daily mean biases at CrIS SWIR channel 1293 (2520.0 cm^{-1}) at nighttime. This is a shortwave window channel, which observes the sea surface temperature over clear sky. Only nighttime results are shown here to reduce the large uncertainty from the simulation due to the potential strong solar reflection contribution and potential sun glint over the ocean during the daytime. Bias1 and Bias2 show very similar short-term variation from day to day with absolute bias less than −0.4 K, but Bias2 shows better long-term stability than Bias1. Results showed in Figs. 5–7 demonstrate that when evaluated using ERA-interim data, CrIS reprocessed SDRs have very high long-term stability, which is one of the most important requirements for reanalysis and climate applications.

The uniformity of FOV-to-FOV radiometric performance is significantly improved in the CrIS reprocessed SDRs due to the improvement of the NL coefficients, which can be seen in Fig. 8. Fig. 8 shows the time series of the longwave daily mean FOV-to-FOV difference (17 channels averaged from 670 to 680 cm^{-1}) with respect to the center FOV 5 for the clear sky over the ocean. The top panel shows the results from the operational IDPS SDRs, while the bottom

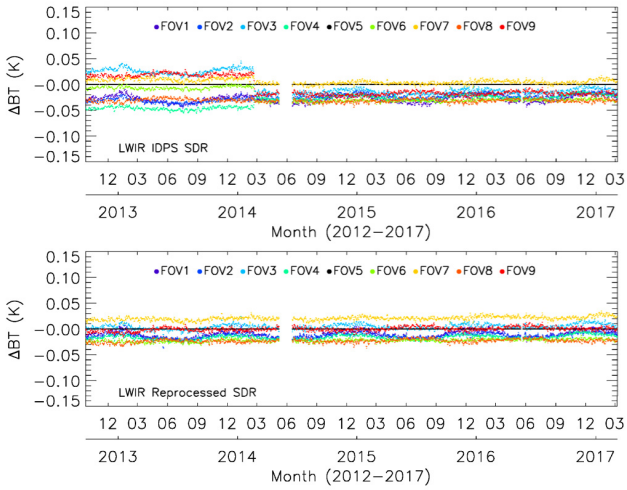

Fig. 8. Time series of the LWIR band daily mean FOV-to-FOV difference (17 channels averaged from 670 to 680 cm^{-1}) with respect to the center FOV 5 for clear sky over ocean.

Fig. 9. Time series of the MWIR band daily mean FOV-to-FOV difference (13 channels averaged from 1585 to 1600 cm^{-1}) with respect to the center FOV 5 for clear sky over ocean.

panel shows the results from the reprocessed SDRs. The FOV-to-FOV difference becomes much tighter and smaller in the reprocessed SDRs than the operational IDPS SDRs before February 20, 2014, and shows very high consistency and stability during the reprocessing period with difference ranging from −0.03 to 0.03 K. The high agreement among the nine FOVs in radiometric performance allows the NWP and reanalysis models to assimilate CrIS data from all of the FOVs without special treatment for different FOVs. Fig. 9 shows the time series of the MWIR band daily mean FOV-to-FOV difference (13 channels averaged from 1585 to 1600 cm^{-1}) with respect to the center FOV 5. One can see some improvements in the FOV-to-FOV radiometric performance and more consistency for the reprocessed SDRs due to the calibration algorithm update [using (2) instead of (1)], the dynamically updated resampling matrix, and the FOV 7 NL coefficient update (see Fig. 1) compared with the operational IDPS

SDRs. At SWIR spectral regions, the FOV-to-FOV radiometric performance of the reprocessed data is nearly identical to the operational one (not shown here) since SWIR band detectors are linear.

C. Spectral Accuracy and Stability

The CrIS radiometric accuracy depends on the accuracy of the spectral calibration. As shown in [13], the BT impact from the unapodized spectra can be as large as 0.25 K at LWIR CO_2 strong absorption channels, a very critical region to derive temperature profiles in retrieval and data assimilation systems, when the spectral shift is 4 ppm. Improving the spectral accuracy and stability is very important to reduce the CrIS observation radiometric uncertainty and potentially improve the climate trend derived from the climate systems when CrIS data is used.

There are two basic spectral assessment methods to evaluate spectral accuracy [12], [13], [30]. The first one is the absolute method, which requires an accurate forward model to simulate the top of atmosphere radiance spectra under clear conditions. The final spectral shift in units of ppm can be determined at the maximum correlation between the observed spectra to the simulated spectra by shifting the spectra at a certain range, from either the observation or the simulation. The second method is the relative method. It does not require the simulation from a forward model, it only requires two uniform observations to determine the spectral offset relative to each other.

Following [13], the absolute method is used to assess the spectral accuracy and stability for both the reprocessed SDRs and the operational IDPS SDRs. Fig. 10 shows the LWIR band long-term spectral accuracy and stability for the reprocessed CrIS SDRs (red line with an open circle), compared to the operational IDPS SDRs (green line with an open circle). The relative variations of the metrology laser wavelength measured by the neon calibration system (blue line, indicated by "Neon Cal") are also included. In this case, the absolute spectral error is derived from comparisons between the spectral performance of the CrIS SDR against CRTM model simulations using ECMWF forecast data, for FOV 5. The comparisons were limited at nadir observations (FORs 15 or 16) with daily average applied when observations were in descending orbit and over clear tropical ocean scenes. Choosing the descending orbit (nighttime) to perform the spectral error evaluation was mainly to reduce the uncertainty from the forward model simulation over daytime with more dynamic surface and atmospheric conditions. The three vertical dashed lines in this figure correspond to three major events (CMO update, IDPS software upgrade, or instrument change): February 20, 2014 (IDPS Mx8.1, validated status), December 4, 2014 (full spectral interferogram mode implemented in RDR data), and March 8, 2017 (IDPS Block 2.0 Mx1, both FSR and NSR products operational). It is shown that CrIS relative metrology laser wavelength varies within 4 ppm (ranging from −2.5 to 1.5 ppm) as measured by the neon calibration system from February 21, 2012 to December 15, 2018. Note that the relative metrology laser wavelength variation

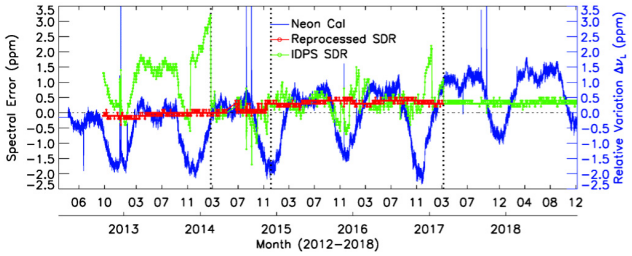

Fig. 10. LWIR band long-term spectral accuracy and stability for reprocessed CrIS SDRs (red line with open circle), compared to operational IDPS SDRs (green line with open circle), and neon calibration system (blue line, indicated by "Neon Cal"). The absolute spectral error using RT model is for the daily average of FOV 5 at nadir (FORs 15 or 16), descending orbit over clear tropical ocean scenes. The three vertical dashed lines are for major events (CMO update, IDPS software upgrade, or instrument change): February 20, 2014 (IDPS Mx8.1, validated status), December 4, 2014 (full spectral interferogram mode implemented in RDR data), and March 8, 2017 (IDPS Block 2.0 Mx1, both FSR and NSR products operational).

on December 19, 2012 (zero spectral shift) is using as a reference. This is the date when the CMO was updated with a new metrology laser wavelength which exceeded 2 ppm threshold compared to the saved previous metrology laser wavelength. The CrIS relative variation of the metrology laser wavelength shows a seasonal pattern, primarily associated with changes in the laser diode temperature. The relative metrology wavelength variations showed a slight upward trend of about 0.25 ppm per year. In the CrIS instrument spectral calibration system, the laser diode temperature is highly correlated with the metrology laser wavelength. The relative metrology wavelength variation trend of 0.25 ppm per year would be caused by the gradually degraded laser diode temperature in the system. Due to software updates and bug fixes, as well as the ILS calibration coefficients updates in the EP, the actual spectral error from the operational IDPS SDRs is about 4 ppm from peak to peak before March 8, 2017, with unpredictable characteristics, especially before February 20, 2014. Although the CrIS processing system was designed to update the resampling matrix after the metrology wavelength exceeds cumulative variations of 2 ppm. However, during this period, results reported in Fig. 10 show that the spectral errors are not following the relative changes of the metrology laser wavelength, as was expected. After March 8, 2017, the spectral errors from the operational IDPS SDRs are at the same level as the spectral errors from the reprocessed SDRs. This is mainly due to the more frequent updates of the resampling matrix using the measured metrology laser wavelength given by the neon calibration system every 109 min (see Section II-B and Table I for further details). As a contrast, the spectral errors derived from the reprocessed SDRs are significantly reduced to less than 0.5 ppm with very high long-term stability. With dynamically updated resampling matrix using the metrology laser wavelength, the trend of 0.25 ppm per year was effectively removed in the CrIS reprocessed SDR data. However, a slight upward trend in the spectral errors (∼0.1 ppm per year) from the reprocessed SDRs was observed. Different from the trend from the relative metrology laser wavelength controlled by the slowly increased interferometer baseplate temperature

TABLE II
OVERALL QUALITY PERFORMANCE OF SNPP CRIS NSR SDR REPROCESSING DATA

Band		LW	MW	SW
Spectral Range (cm^{-1})		650-1095	1210-1750	2155-2550
Number of Channels		713	433	159
Spectral Resolution (cm^{-1})		0.625	1.25	2.5
NedN* @287K BB $mW/m^2/sr/cm^{-1}$	Specification	0.14	0.06	0.007
	Operational Validated SDR	0.098	0.036	0.003
	Reprocessed SDR	0.098	0.036	0.003
Radiometric Uncertainty* @287K BB (%)	Specification	0.45	0.58	0.77
	Operational Validated SDR	0.16	0.19	0.40
	Reprocessed SDR	0.16	0.19	0.40
Spectral Uncertainty (ppm)	Specification	10	10	10
	Operational Validated SDR	3	3	3
	Reprocessed SDR	2	2	2
Geolocation Uncertainty** (km)	Specification	1.5	1.5	1.5
	Operational Validated SDR	1.2	1.2	1.2
	Reprocessed SDR	0.25	0.25	0.25

*Based on S-NPP CrIS validated SDR data after 02/20/2014
**Geolocation Uncertainty based on LW band

and laser diode temperature, this trend may indicate the slow degradation of the effective neon wavelength in the CrIS neon calibration system including the electrical and optical changes around the laser diode and is difficult to remove in the ground processing system. Assuming the trend continues during a 10-year period, a 1-ppm spectral calibration error would be expected for the CrIS reprocessed SDR data product. This trend should have an impact on of less than 0.03 and 0.01 K for unapodized and Hamming-apodized spectra, respectively. The impact is mainly expected around strong atmospheric absorption channels, such as the temperature-sounding channels located at 650–770 cm^{-1} over the CrIS LWIR band, and over the whole water vapor channels found at the CrIS MWIR band. This means that the CrIS reprocessed data holds small radiometric errors of less than 0.03 K per decade, associated with spectral calibration errors. This performance is adequate and is in line with the radiometric stability requirement needed for climate applications, which is about (0.04 K per decade) [31] and was particularly established to derive climate trend such as CO_2 concentration, temperature and water vapor from the CrIS reprocessed SDRs.

The time series of all the FOVs spectral accuracy for the reprocessed data is shown in Fig. 11. The overall mean spectral error (black line) and standard deviation (red lines) are also included. It shows that the spectral error trends from other FOVs are very similar to that from FOV 5, all about 0.1 ppm per year. The spectral spread is very stable, less than 0.6 ppm with FOV 9 having the largest error (mean 0.74 ppm) and FOV 5 smallest error (mean 0.16 ppm). The overall mean spectral error is 0.43 ppm over all the FOVs with a standard deviation of 0.55 ppm.

D. Overall Performance of the Reprocessed Data

The overall quality performance of the reprocessed SDR data is summarized in Table II. This table listed the

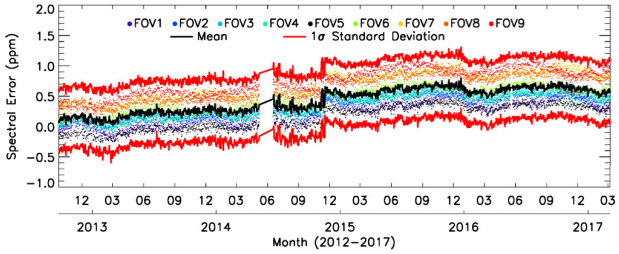

Fig. 11. Time series of the LWIR band daily mean absolute spectral accuracy and stability for reprocessed CrIS SDR data for all nine FOVs (indicated by difference color dots) over clear tropical ocean scenes. The center FOV 5 result is same as in Fig. 10. The mean spectral accuracy over nine FOVs is indicated by black line, and the two red lines are the mean value plus/minus standard deviation.

reprocessed SDR data performance in terms of noise, radiometric, spectral as well as geolocation uncertainty. Compared to the operational validated SDR products, the reprocessed SDR data have smaller spectral and geolocation errors, improved from 3 to 2 ppm, and 1.2 to 0.25 km, respectively. Although the radiometric uncertainty does not improve, the long-term stability and consistency are significantly improved for the reprocessed SDR data. Based on the overall performance, the reprocessed SDR data can be used for long-term climate monitoring and model assessments, and provide an IR reference observation to assess other narrow- or broadband IR instruments' calibration accuracy.

IV. CONCLUSION

Since the launch of the S-NPP satellite, the CrIS instrument has provided more than seven years of measurements. In the process of achieving different maturity stages, the operational CrIS SDR data generated in real-time from IDPS software is continuously improved due to the updates of the processing software system as well as the calibration coefficients. Consequently, the operational SDR data may have varying

characteristics affecting the long-term stability in terms of radiometric, spectral, as well as geolocation performance. In this study, the CrIS SDR data is improved for climate applications with its optimized and improved calibration coefficients. One specific software system for the baseline CrIS SDR reprocessing was developed. This software system was updated with the calibration algorithm, NL, and geolocation to improve the CrIS SDR data quality and long-term consistency. The calibration coefficients are refined with the latest updates, which were used to calibrate the latest operational SDR products. Those refined coefficients were incorporated in the EP of the RDR data stream used to generate the reprocessed CrIS SDR data.

The CrIS radiometric and spectral calibration was assessed in terms of its accuracy and stability, using comparisons between the reprocessed SDR data and the operational IDPS SDR data. The overall radiometric biases are small (channel dependent) and stable over time, FOV-to-FOV differences are less than ∼10 mK and much better than that from the operational IDPS SDR. It is shown that CrIS metrology laser wavelength varies within 4 ppm as measured by the neon calibration system. The reprocessed SDR data shows significant improvements with respect to the operational data, with spectral errors of less than 0.5 ppm over more than 4 years. The operational IDPS SDR data holds spectral errors of up to 4 ppm within the same period.

The baseline reprocessed CrIS SDR data, which has shown better radiometric and spectral calibration accuracy, as well as consistent calibration stability, relies on a single and dedicated processing system with improved calibration coefficients. This system can be used to generate high-quality reprocessed CrIS SDR data, adequate for long-term climate monitoring and model assessment applications. It is expected that this data set also supports instrument inter-calibration activities and be considered as an on-orbit IR observation reference to assess the calibration accuracy of observations from other hyperspectral and multispectral IR instruments.

ACKNOWLEDGMENT

The authors would like to thank the JPSS CrIS Science team for supporting the work that is summarized in this article and to acknowledge the hard work and dedication of all contributing individual companies and organizations from the CrIS SDR science team. The authors thank Dr. Peter Beierle and three anonymous reviewers for providing constructive comments to improve this article.

Disclaimer: The scientific results and conclusions, as well as any views or opinions expressed herein, are those of the author(s) and do not necessarily reflect those of NOAA or the Department of Commerce and the U.S. Government.

REFERENCES

[1] Y. Han and Y. Chen, "Calibration algorithm for cross-track infrared sounder full spectral resolution measurements," *IEEE Trans. Geosci. Remote Sens.*, vol. 56, no. 2, pp. 1008–1016, Feb. 2018.

[2] J. Le Marshall *et al.*, "Improving global analysis and forecasting with AIRS," *Bull. Amer. Meteorol. Soc.*, vol. 87, pp. 891–894, Jul. 2006.

[3] F. Hilton *et al.*, "Hyperspectral Earth observation from IASI," *Bull. Am. Meteorol. Soc.*, vol. 93, no. 3, pp. 347–370, Mar. 2012.

[4] R. Eresmaa, J. Letertre-Danczak, C. Lupu, N. Bormann, and A. P. McNally, "The assimilation of cross-track infrared sounder radiances at ECMWF," *Quart. J. Roy. Meteorol. Soc.*, vol. 143, no. 709, pp. 3177–3188, Oct. 2017.

[5] H. H. Aumann and T. S. Pagano, "Using AIRS and IASI data to evaluate absolute radiometric accuracy and stability for climate applications," in *Atmospheric and Environmental Remote Sensing Data Processing and Utilization Iv: Readiness for Geoss Ii*, vol. 7085, M. D. Goldberg, H. J. Bloom, P. E. Ardanuy, and A. H. L. Huang, Eds. San Diego, CA, USA: The International Society for Optics and Photonics, 2008.

[6] N. Smith, W. L. Smith, E. Weisz, and H. E. Revercomb, "AIRS, IASI, and CrIS retrieval records at climate scales: An investigation into the propagation of systematic uncertainty," *J. Appl. Meteorol. Climatol.*, vol. 54, no. 7, pp. 1465–1481, Jul. 2015.

[7] L. Wang and C. Cao, "On-orbit calibration assessment of AVHRR longwave channels on MetOp–A using IASI," *IEEE Trans. Geosci. Remote Sens.*, vol. 46, no. 12, pp. 4005–4013, Dec. 2008.

[8] M. Goldberg *et al.*, "The global space-based inter-calibration system," *Bull. Amer. Meteorol. Soc.*, vol. 92, no. 4, pp. 467–475, Apr. 2011.

[9] L. Wang, Y. Han, X. Jin, Y. Chen, and D. A. Tremblay, "Radiometric consistency assessment of hyperspectral infrared sounders," *Atmos. Meas. Techn.*, vol. 8, no. 11, pp. 4831–4844, Nov. 2015.

[10] Y. Han *et al.*, "Suomi NPP CrIS measurements, sensor data record algorithm, calibration and validation activities, and record data quality," *J. Geophys. Res., Atmos.*, vol. 118, no. 22, pp. 12734–12748, Nov. 2013.

[11] D. Tobin *et al.*, "Suomi-NPP CrIS radiometric calibration uncertainty," *J. Geophys. Res., Atmos.*, vol. 118, pp. 10589–10600, Sep. 2013.

[12] L. L. Strow *et al.*, "Spectral calibration and validation of the cross-track infrared sounder on the Suomi NPP satellite," *J. Geophys. Res., Atmos.*, vol. 118, no. 22, pp. 12486–12496, Nov. 2013.

[13] Y. Chen, Y. Han, and F. Weng, "Characterization of long-term stability of suomi NPP cross-track infrared sounder spectral calibration," *IEEE Trans. Geosci. Remote Sens.*, vol. 55, no. 2, pp. 1147–1159, Feb. 2017.

[14] L. Wang *et al.*, "Geolocation assessment for CrIS sensor data records," *J. Geophys. Res. Atmos.*, vol. 118, no. 22, pp. 12690–12704, 2013.

[15] L. Wang, B. Zhang, D. Tremblay, and Y. Han, "Improved scheme for cross-track infrared sounder geolocation assessment and optimization," *J. Geophys. Res., Atmos.*, vol. 122, no. 1, pp. 519–536, Jan. 2017, doi: 10.1002/2016JD025812.

[16] V. Zavyalov *et al.*, "Noise performance of the CrIS instrument," *J. Geophys. Res., Atmos.*, vol. 118, no. 23, pp. 13108–13120, Dec. 2013.

[17] Y. Chen, F. Weng, and Y. Han, "SI traceable algorithm for characterizing hyperspectral infrared sounder CrIS noise," *Appl. Opt.*, vol. 54, no. 26, pp. 7889–7894, Sep. 2015.

[18] H. Revercomb, H. Buijs, and H. Howell, "Radiometric calibration of IR Fourier transform spectrometers: Solution to a problem with the high-resolution interferometer sounder," *Appl. Opt.*, vol. 27, pp. 273210–273218, Aug. 1988.

[19] H. Revercomb, and Coauthors, "CrIS ringing artifacts: Progress on implementing a correction," in *Proc. Weekly CrIS Calibration/Validation Teleconf.*, Sep. 2014, pp. 1–9.

[20] J. Predina *et al.*, "Future JPSS cross-track infrared sounder (CrIS) ground algorithm improvements," in *Proc. OSA Hyperspectral Imag. Sounding Environ. (HISE) Conf.*, vol. 2, Mar. 2015, pp. 1–4.

[21] J. Genestand and P. Tremblay, "Instrument line shape of Fourier transform spectrometers: Analytic solutions for nonuniformly illuminated off-axis detectors," *Appl. Opt.*, vol. 38, pp. 5438–5446, Sep. 1999.

[22] Y. Han, L. Suwinski, D. Tobin, and Y. Chen, "Effect of self-apodization correction on cross-track infrared sounder radiance noise," *Appl. Opt.* vol. 54, no. 34, pp. 10114–10122, Dec. 2015, doi: 10.1364/AO.54.010114.2015.

[23] *Joint Polar Satellite System (JPSS) Cross Track Infrared Sounder (CrIS) Sensor Data Records (SDR) Algorithm Theoretical Basis Document (ATBD) for Normal Spectral Resolution*, document E/RA-00002, 2018. [Online]. Available: https://www.star.nesdis.noaa.gov/jpss/documents/ATBD/D0001-M01-S01-002_JPSS_ATBD_CRIS-SDR_nsr_20180614.pdf

[24] L. Wang, D. Tremblay, B. Zhang, and Y. Han, "Fast and accurate collocation of the visible infrared imaging radiometer suite measurements with cross-track infrared sounder," *Remote Sens.*, vol. 8, no. 1, p. 76, Jan. 2016, doi: 10.3390/rs8010076.

[25] L. Wang and Y. Chen, "Inter-comparing SNPP and NOAA-20 CrIS toward measurement consistency and climate data records," *IEEE J. Sel. Topics Appl. Earth Observ. Remote Sens.*, vol. 12, no. 7, pp. 2024–2031, Jul. 2019, doi: 10.1109/JSTARS.2019.2891701.

[26] Y. Chen, F. Weng, Y. Han, and Q. Liu, "Validation of the community radiative transfer model by using CloudSat data," *J. Geophys. Res.*, vol. 113, no. D00A03, pp. 1–15, 2008, doi: 10.1029/2007JD009561.

[27] Y. Chen, Y. Han, P. Van Delst, and F. Weng, "On water vapor Jacobian in fast radiative transfer model," *J. Geophys. Res.*, vol. 115, no. D12303, pp. 1–20, 2010, doi: 10.1029/2009JD013379.

[28] Y. Chen, Y. Han, P. van Delst, and F. Weng, "Assessment of shortwave infrared sea surface reflection and nonlocal thermodynamic equilibrium effects in the community radiative transfer model using IASI data," *J. Atmos. Ocean. Technol.*, vol. 30, no. 9, pp. 2152–2160, Sep. 2013.

[29] D. P. Dee *et al.*, "The ERA-interim reanalysis: Configuration and performance of the data assimilation system," *Quart. J. Roy. Meteorol. Soc.*, vol. 137, no. 656, pp. 553–597, Apr. 2011, doi: 10.1002/qj.828.

[30] Y. Chen, Y. Han, and F. Weng, "Detection of Earth-rotation Doppler shift from Suomi national polar-orbiting partnership cross-track infrared sounder," *Appl. Opt.*, vol. 52, pp. 6250–6257, Dec. 2013.

[31] G. Ohring, B. Wielicki, R. Spencer, B. Emery, and R. Datla. (2004). *Satellite Instrument Calibration for Measuring Global Climate Change*. [Online]. Available: http://physics.ist.gov/Divisions/Div844/publications/NISTIR7047/nistir7047.pdf

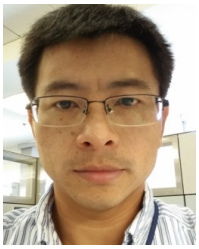

Yong Chen received the B.S. and M.S. degrees in atmospheric sciences from Peking University, Beijing, China, in 1996 and 1999, respectively, and the Ph.D. degree in atmospheric sciences from the University of California, Los Angeles, CA, USA, in 2005.

He is a Physical Scientist with NOAA/NESDIS/Center for Satellite Applications and Research, College Park, MD, USA. His research interests include: radiative transfer theory and applications; development and implementation of fast radiative transfer model for satellite data assimilation; radiometric and spectral calibration and validation of satellite hyperspectral infrared sounders, IR data process; and Global Navigation Satellite System Radio Occultation data processing and data assimilation.

Flavio Iturbide-Sanchez (Senior Member, IEEE) received the B.S.E.E. degree in electronics engineering from Autonomous Metropolitan University, Mexico City, Mexico, in 1999, the M.S.E.E. degree in electrical engineering from the Advanced Studies and Research Center, National Polytechnic Institute, Mexico City, in 2001, and the Ph.D. degree from the University of Massachusetts, Amherst, MA, USA, in 2007. His Ph.D. research focused on the miniaturization, development, calibration, and performance assessment of low-cost and power-efficient microwave radiometers for remote sensing applications.

From 2001 to 2005, he was a Research Assistant with Microwave Remote Sensing Laboratory, University of Massachusetts, where he was involved in the design, development, and characterization of highly integrated multichip modules and microwave circuits for low-noise, low-power consumption, high-gain, and high-stability microwave radiometers. From 2005 to 2007, he was with the Microwave Systems Laboratory, Colorado State University, Fort Collins, CO, USA, focusing on the demonstration of a low-cost and power-efficient compact microwave radiometer for humidity profiling. From 2008 to 2018, he supported the development of operational physical retrieval systems that employ hyperspectral-infrared and microwave observations implemented for the Polar Operational Environmental Satellites Project (POES) and the Joint Polar Satellite System (JPSS). He has been a Physical Scientist with NOAA/NESDIS/Center for Satellite Applications and Research, College Park, MD, USA, since 2018, where he has led the calibration and validation of the JPSS Cross-track Infrared Sounder instruments and supports the planning of the next generation of NOAA infrared and microwave sounders. His research interests include satellite remote sensing, satellite data assimilation, inverse theory applied to geoscience fields, weather forecasting, Earth system science, small satellites, and the design of radiometer systems for Earth observations based on emerging technologies.

Denis Tremblay received the Ph.D. degree in aerospace engineering from the University of Colorado, Boulder, CO, USA, in 1995.

He has been a member of the CrIS team since 2006. He contributed to software development with emphasis on the calibration (SDR), geolocation, simulation, integration, testing, and science validation.

David Tobin received the B.S., M.S., and Ph.D. degrees in physics from the University of Maryland, Baltimore, MD, USA in 1991, 1993, and 1996, respectively.

He is a Distinguished Scientist at the Cooperative Institute for Meteorological Satellite Studies (CIMSS) within the Space Science and Engineering Center (SSEC) at the University of Wisconsin-Madison, Madison, WI, USA. His research interests include infrared molecular spectroscopy, infrared radiative transfer, hyperspectral sensor design, calibration, and data processing, and satellite inter-calibration.

Dr. Tobin is a member of the International Radiation Commission, the Global Space-based Inter-Calibration System (GSICS) Research Working Group, and the International TOVS Advanced Sounder Working Group.

Larrabee Strow, photograph and biography not available at the time of publication.

Likun Wang received the B.S. degree in atmospheric sciences and the M.S. degree in meteorology from Peking University, Beijing, China, in 1996 and 1999, respectively, and the Ph.D. degree in atmospheric sciences from the University of Alaska Fairbanks, Fairbanks, AK, USA, in 2004.

He serves the Chair of World Meteorological Organization (WMO) sponsored Global Space-based Inter-Calibration System (GSICS) infrared sensor working group. He is working as a Visiting Scientist affiliated with NOAA/NESDIS/STAR and employed by the Earth System Science Interdisciplinary Center at the University of Maryland.

Daniel L. Mooney is a Senior Staff Member in the Sensor Technology and System Applications group at MIT Lincoln Laboratory, Lexington, MA, USA. He has worked in a wide variety of programs in many years at Lincoln Laboratory including infrared instrument design and calibration.

Dr. Mooney is working with NOAA and NASA in the development of NPP and JPSS infrared remote sounding instruments for the current polar orbit weather satellites.

David Johnson is a Senior Instrument Scientist in the Engineering Directorate at NASA Langley Research Center. He is the NASA Instrument Scientist for CrIS series of instruments on the JPSS polar orbiting weather satellites, and has previously served as the technical lead on a number of NASA projects, including the infrared spectrometer on CLARREO, the INFLAME instruments, the FIRST instrument, and the EVA IR Camera. He has 34 years of experience in atmospheric remote sensing and instrument development and is the author or coauthor of 49 peer reviewed publications and numerous other publications and presentations.

Joe Predina is the President of Logistikos Engineering, Fort Wayne, IN, USA, a small aerospace engineering firm that specializes in the research and development of remote sensor technology for space instruments.

Mr. Predina previously was a Tech Fellow at the L3Harris Corporation where he was systems engineer on the CrIS and GOES instrument programs.

Lawrence Suwinski, photograph and biography not available at the time of publication.

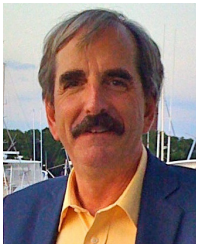

Henry (Hank) E. Revercomb is Senior Scientist and Director (1999–2016), Space Science and Engineering Center (SSEC), University of Wisconsin-Madison, Madison, WI, USA, and involved in using radiation measurements to study the atmospherics of Earth and other planets. His research interest includes high spectral resolution instrumentation for atmospheric remote sensing and spectroscopy, operational temperature and water vapor sounders, climate observing systems, and net radiative flux observations of Venus and Jupiter.

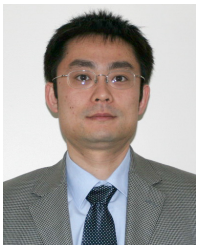

Ninghai Sun received the Ph.D. degree in atmospheric remote sensing from the University of Maryland, College Park, MD, USA, in 2009. Since 2002, he has worked at NOAA Center for Satellite Application and Research as a research scientist. He is the Technical Lead of Advanced Technology Microwave Sounder (ATMS) Calibration/Validation team. His major activities focus on the development of operational satellite microwave instrument calibration theory and remote sensing application retrieval algorithms. He is a Senior Project Engineer/Scientist to develop the JPSS lifecycle reprocessing system for ATMS, CrIS, and OMPS.

Dr. Sun is also the creator of the STAR operational Integrated Cal/Val System (ICVS), which is a real time and long term NOAA, NASA, and EUMETSAT meteorological satellites operational status monitoring and calibration system to support NOAA daily operational missions. He is also a member of Global Space-based Inter-Calibration System (GSICS) of World Meteorological Organization (WMO) to develop inter-satellite calibration algorithm and data product for climate study.

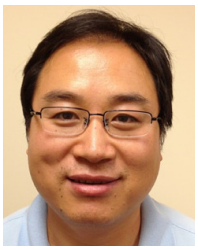

Bin Zhang received the B.S. degree in geophysics from the University of Science and Technology of China, Hefei, China, in 1996, the M.S. degree in physical oceanography from the Institute of Oceanology, Chinese Academy of Science, Qingdao, China, in 1999, and the Ph.D. degree in oceanography from Old Dominion University, Norfolk, Virginia, USA, in 2008.

He is an Assistant Research Scientist with the University of Maryland, College Park, MD, USA. He has supported work on calibration/validation/reprocessing for SNPP/NOAA-20 VIIRS instrument and on VIIRS/CRIS geolocation validation, the Advanced Microwave Radiometer validation for Jason series satellites, and algorithm development for GNSS Radio Occultation (COSMIC-2 and other missions).

Changyong Cao received the B.S. degree in geography from Peking University, Beijing, China, in 1982 and the Ph.D. degree in geography specializing in remote sensing from Louisiana State University, Baton Rouge, LA, USA, in 1992.

He is a Research Physical Scientist with the NOAA Center for Satellite Applications and Research. He specializes in the calibration of radiometers onboard NOAA's Operational Environmental Satellites. In his early career with NOAA, he has served as the infrared sounder instrument scientist, and leads the VIIRS sensor science team. He has made significant contributions to the international and interagency satellite community, including the Committee on Earth Observation Satellites (CEOS) and World Meteorological Organization Global Space-based Inter-Calibration System (GSICS). Before joining NOAA in 1999, he was a Senior Scientist with five years of aerospace industry experience supporting NASA projects.

Dr. Cao was the recipient of three gold and one silver medals honored by the U.S. Department of Commerce for his scientific and professional achievements.

Satya Kalluri received the M.Sc. degree in geography from Osmania University, Hyderabad, India, in 1990, and the Ph.D. degree from the University of Maryland, College Park, MD, USA, in 1994.

He is the Chief of the Satellite Meteorology and Climatology division at NOAA/NESDIS/STAR and the acting chief scientist of the Joint Polar Satellite System. His main interests are in developing satellite data applications for land and atmospheric studies. At NOAA, he managed the development of algorithms for processing science data from GOES-R, JPSS, and MetOp-SG missions in to ocean, land and atmospheric products.

Lihang Zhou worked on GOES-R as the quality assurance manager for the algorithm working group (AWG) from 2006 to 2009. From 2009 to 2011 she worked in NOAA Integrated Program Office (IPO) as the Senior Data Product and Algorithm Scientist. Before joining JPSS, she worked at NOAA/STAR as the STAR JPSS Program Manager and the science deputy for the JPSS Algorithm Management Project. She is the Data Products Management and Services (DPMS) Deputy and the Products Portfolio Manager in NOAA Joint Polar Satellite System (JPSS). She has extensive experience on satellite algorithm development, calibration/validation, and program management. She has also worked on algorithm development for retrieving products from the hyperspectral infrared sounding instruments onboard the U.S. and international satellites.